A Full-Stack Open-Source Framework for Antenna and Beamforming Evaluation in mmWave 5G NR

Mattia Lecci, Tommaso Zugno, Silvia Zampato, Michele Zorzi

Department of Information Engineering, *University of Padova*, Italy

{name.surname@dei.unipd.it}

Abstract—**Millimeter wave (mmWave) communication represents one of the main innovations of the next generation of wireless technologies, allowing users to reach unprecedented data rates. To overcome the high path loss at mmWave frequencies, these systems make use of directional antennas able to focus the transmit power into narrow beams using BeamForming (BF) techniques, thus making the communication directional. This new paradigm opens up a set of challenges for the design of efficient wireless systems, in which antenna and BF components play an important role also at the higher layer of the protocol stack. For this reason, accurate modeling of these components in a full-stack simulation is of primary importance to understand the overall system behavior.**

This paper proposes a novel framework for the end-to-end simulation of 5G mmWave cellular networks, including a ray-tracing based channel model and accurate models for antenna arrays and BF schemes. We showcase this framework by evaluating the performance of different antenna and BF configurations considering both link-level and end-to-end metrics and present the obtained results.

Index Terms—**mmWave, antenna, beamforming, 5G, NR, ns-3**

I. INTRODUCTION

One of the focus points of the next generation of wireless networks is the use of the mmWave band, often identified with frequencies between 6 and 100 GHz. Thanks to the amount of available bandwidth that characterizes this portion of the spectrum, wireless systems that operate at mmWave frequencies can use much wider bandwidths compared to legacy technologies. As a result, users can obtain unprecedented data rates, in the order of gigabits-per-second, paving the way for new advanced use cases such as virtual and augmented reality. 3GPP NR [1], the communication standard for the 5G of cellular networks, currently supports carrier frequencies up to 52.6 GHz, with possible extensions to 71 GHz in future releases [2].

Radio Frequency (RF) signals at mmWave frequencies, though, present some additional difficulties with respect to their more common sub-6 GHz counterpart [3]. For example, free space propagation loss increases significantly, making wireless links harder to maintain over long distances. This, in turn, tends to dissipate high-order reflections and diffractions, making the mmWave channel sparser and more directional,

reducing both intra-cell and inter-cell interference, thus allowing spatial diversity among different users. Furthermore, the higher penetration loss occurring in common materials, as well as a deeper diffraction shadow, make it much harder to maintain a reliable connection in Non Line of Sight (NLOS) conditions. Finally, the shorter wavelength results in a lower channel coherence time in mobile environments, making the connection less stable due to the rapid channel fluctuations.

Using directive antennas, especially in the form of electronically steered phased antenna arrays, can solve most of the problems caused by the physics of the mmWave band. In fact, directivity can compensate for the higher propagation loss by focusing the power into narrow beams, thus restoring the possibility of medium-range transmissions, while also further reducing interference and the contribution of secondary paths to the receiver, thus improving the channel coherence time [4] and the aggregated cell performance.

On the other hand, directional communications make it inherently more difficult to handle mobile scenarios, making it necessary to keep the alignment between the transmitter and receiver beams [5], introducing more overhead. Directivity is even more critical when experiencing sudden blockage events. In this case, the pair of communicating devices should either store backup links or find a new connection on the fly, increasing the overhead and complexity of beam management operations.

The combination of these phenomena may seriously affect the quality experienced by mobile users. In this context, it is necessary to implement a detailed performance evaluation to identify and address the weakest points of the technology across the full communication stack. Cellular networks are extremely complex systems, highly correlated with hidden factors that can impact the overall performance at different scales. Usually, the different components, i.e., the antenna system, the RF components, the cellular protocol stack, etc., are designed using a block-level approach, developing each block independently of the others. However, this methodology may lead to undesired behaviors and even sub-optimal performance, since the possible side effects among the components may have a strong impact on the overall system. This problem can be solved using system-level simulation tools, which represent an accurate and cheap solution to evaluate the overall performance before the actual deployment and to adjust the design of each component accordingly. Indeed, simulation enables large scale evaluations, allowing the user to decide

the degree of abstraction required by the desired analysis [6].

In this work, we showcase an open-source and publicly available [1] framework for full-stack 5G NR-compliant simulations, based on the popular open-source Network Simulator 3 (ns-3). While other 5G NR simulators already exist, to the best of our knowledge we propose a simulator with (i) a ray-tracing based channel model for mobile users, improving the spatio-temporal coherence over the previous stochastic channel [7], (ii) a flexible antenna module, comprising of multiple parametric antenna elements as well as a generic interface for phased antenna arrays, and (iii) a BF module. This work builds on top of a pre-existing full-stack 5G NR mmWave simulator [8], a popular tool developed jointly by the University of Padova and NYU-Wireless. Thanks to the integration with ns-3, this simulator features a detailed implementation of the TCP/IP stack, together with several traffic and mobility models, allowing the community to analyze and compare full-stack behaviors of different physical and protocol setups.

This paper is organized as follows. In Section II, we describe the feature we developed to enable a more realistic modeling of the mmWave channel. In Section III, we present new simulation models for antenna arrays and BF. In Section IV we show the simulation setup used to obtained the results for Section V. Finally, in Section VI we conclude and propose future developments for this work.

II. CHANNEL MODELING

When simulating wireless networks, channel modeling plays a key role to make simulations more realistic, and this is even more important when simulating mmWave links [9]. Some key features differentiate a mmWave link with respect to a sub-6 GHz link, specifically (i) the higher propagation loss, (ii) the spatial sparsity, (iii) the higher penetration losses and deep diffraction shadows, and (iv) the more prominent diffuse scattering [10].

While propagation losses are usually based on simple models, the other characteristics make the mmWave channel more complicated to both simulate and manage. For example, spatial sparsity, together with mobile users and directional antennas, require a realistic spatio-temporal correlation to simulate realistic results, especially when beam-tracking techniques need to be evaluated. Furthermore, higher penetration loss and deep diffraction shadows make mmWave suffer from strong blockage due to simple obstacles (e.g., trees, pedestrians, light poles) and even from self-blockage. Finally, diffuse scattering is one of the main causes of fast and frequency-selective fading, which tends to be significant due to the relatively high surface roughness of building materials with respect to the wavelength of the radiated signal.

While stochastic models have proven to be quite accurate for the lower frequencies, these effects are more appropriately taken into account by quasi-deterministic approaches, mixing

deterministic ray-tracing with stochastic models for diffuse scattering [11].

We implemented an add-on for ns-3, making it possible to read channel traces obtained, for example, by a quasi-deterministic mmWave channel simulator. Both the quasi-deterministic channel simulator [12] and the ns-3 add-on [13] are available and open source, making it possible for the community to further improve their results with realistic channel modeling, while keeping the simulation complexity under control [10].

III. ANTENNA ARRAYS AND BEAMFORMING

Antennas are a fundamental component of every wireless system. Given that the size of an antenna is in the order of the wavelength of the desired carrier frequency [14], when operating at mmWave frequencies antennas sizes are in the order of a few millimeters [15], thus allowing to design compact antenna arrays with tens or hundreds of elements.

The most common and scalable approach is the use of phased antenna arrays, which allows us to focus the transmission in the desired direction using coherent interference. By carefully introducing phase shifts to the transmitted signal of each antenna element, it is possible to create complex radiation patterns, a technique called BeamForming (BF). In the simplest case, the overall radiation pattern of the antenna system is computed from the type of antenna element used, the placement of the antenna elements in the 3D space, and the BF scheme used.

Typically, antenna and BF design is carried out as an independent task, by means of real-world experiments or link-level simulations, without considering it as part of the overall system optimization. However, the solutions obtained with this approach may not be able to achieve optimal system-level performance, because they are designed without considering the interactions between the antenna systems and the higher layers of the protocol stack.

To go beyond this standalone block-level design perspective, new tools able to properly consider all the relevant aspects of the cellular system are required. For instance, the authors of [16] verified the importance of carrying out system-level simulations for the design of an 8×8 hybrid beamformer, since the cross effects between the different system blocks may have a strong impact on the overall performance. In [17], the authors present novel antenna array and BF solutions for mmWave Multiple-Input Multiple-Output (MIMO) systems based on lens antennas, and evaluate the end-to-end performance through system level simulations based on ray-tracing. Also, in [18] the authors investigate the possibility of co-designing the antennas and the RF blocks in the front-end using a system-level platform. Although these works tackle antenna and/or BF design with a system-level approach, they make use of closed source software or unavailable tools, specifically developed for a single application.

In this work, we propose new models for the end-to-end performance evaluation of antenna and BF designs targeted for mmWave cellular systems. Thanks to the integration with

---

[1] https://github.com/signetlabdei/ns3-mmwave-antenna

ns-3, these models allow users to evaluate the impact of novel antenna and BF solutions on the end-to-end system behavior. Section III-A describes the antenna array model, Section III-B describes the antenna element model, while Section III-C describes the BF model.

A. Antenna Array Model

Phased antenna arrays can have extremely diverse geometries, from which their BF capabilities are derived. While it would be possible to create a generic class for arbitrary phased arrays, some geometries (e.g., uniform linear and planar arrays) are extremely popular and deserve specialized methods. For this reason, we created a generic interface for phased antenna arrays, specifying the polarized element field pattern, the locations of the elements (from which it is possible to compute the phase difference experienced by each antenna element for a transmitting or receiving signal), and the BF vector (the phase shifts and amplifications applied to every single element necessary to obtain the desired beam shape).

For this work, we considered the model described in the 3GPP specifications TR 38.901 [19]. The standard describes a uniform planar array, meaning that antenna elements are equal and are placed in an equally-spaced $M \times N$ rectangular lattice with vertical spacing d_V and horizontal spacing d_H, which form a panel. In our implementation we consider the simpler case of vertically polarized elements and only a single-panel configuration.

B. Antenna Element Model

Phased antenna arrays are composed of multiple antenna elements capable of radiating and receiving electromagnetic signals. Every antenna element has a specific radiation and polarization pattern due to its specific design. Different antennas are needed in different contexts, e.g., directional elements can be used in multi-sector devices (e.g., Next Generation Node Bases (gNBs)), while quasi-isotropic antennas may be used for devices with no preferred communicating direction (e.g., User Terminals (UTs) with single antenna array).

A huge number of antenna element designs exist in practice, leading us to creating a generic interface allowing users to add their own antenna models. In general, it is possible to create antenna elements with pattern measured from real devices to further increase the simulation accuracy. For this paper, we implemented three of the most common antenna element models, with directivity pattern in dBi D_{dB} in the θ (inclination) and ϕ (azimuth) directions:

- *Isotropic antenna element*

$$D_{\mathrm{dB}}(\theta, \phi) = 0$$

- *3GPP antenna element* [19]

$$D_{\mathrm{v,dB}}(\theta) = -\min\left\{12\left(\frac{\theta - 90°}{\theta_{\mathrm{3dB}}}\right)^2, SLA_V\right\}$$

$$D_{\mathrm{h,dB}}(\phi) = -\min\left\{12\left(\frac{\phi}{\phi_{\mathrm{3dB}}}\right)^2, A_{\max}\right\}$$

$$D_{\mathrm{dB}}(\theta, \phi) = G_{E,\max} - \\ \min\left\{-(D_{\mathrm{v,dB}}(\theta) + D_{\mathrm{h,dB}}(\phi)), A_{\max}\right\}$$

where the side-lobe attenuation in the vertical direction $SLA_V = 30$ dB, the maximum attenuation $A_{\max} = 30$ dB, the vertical and horizontal 3 dB beamwidths are respectively $\theta_{\mathrm{3dB}} = \phi_{\mathrm{3dB}} = 65°$, and the maximum directional gain of the antenna element is $G_{E,\max} = 8$ dBi.

- *Cosine antenna element*

$$D_{\mathrm{dB}}(\theta, \phi) = G_{\max} + \\ 20 \log_{10}\left(\cos^{\alpha_h}\left(\frac{\phi}{2}\right)\cos^{\alpha_v}\left(\frac{90° - \theta}{2}\right)\right),$$

where the exponents $\alpha_{h/v}$ can be computed from the beamwidths $\mathrm{BW}_{h/v}$ as $\alpha_{h/v} = \frac{-3}{20 \log_{10}\cos\frac{\mathrm{BW}_{h/v}}{4}}$, and the maximum gain $G_{\max}$ can be computed from the directivity formula found in [14].

C. Beamforming Model

Multiple BF architectures exist, which are commonly divided into three main categories, namely analog, digital, and hybrid. In analog architectures, a network of phase shifters is used to connect the antenna elements to a single RF chain, enabling a passive control of the beam by acting on the elements' phases. In digital architectures, instead, each antenna element is connected to an independent RF chain to provide digital control of the BF using baseband processing. The presence of multiple RF chains enables Multi-User Multiple-Input Multiple-Output (MU-MIMO) operations, i.e., independent data streams can be transmitted and received simultaneously, possibly serving multiple users at the same time. Finally, hybrid architectures represent a middle ground between analog and digital approaches, in which the array is divided into multiple sections, each including multiple elements connected to an independent RF chain.

Although digital and hybrid architectures have the potential to achieve higher spectral efficiencies, several technological and economic issues still make analog BF a valuable choice, also due to its relatively low complexity. For this reason, in this work we consider the analog architecture and leave the study of the other two categories as future work.

Analog BF is achieved by controlling amplitude and phase shift of each antenna element of the phased array; this corresponds to assigning a complex number to each element, which is often identified as a *BF vector*. Several algorithms exist to compute such vectors, each affecting the directivity pattern in a unique way. Some try to maximize the gain in given directions, some try to suppress side lobes, some try to regulate the beamwidth, some others try to optimize the performance
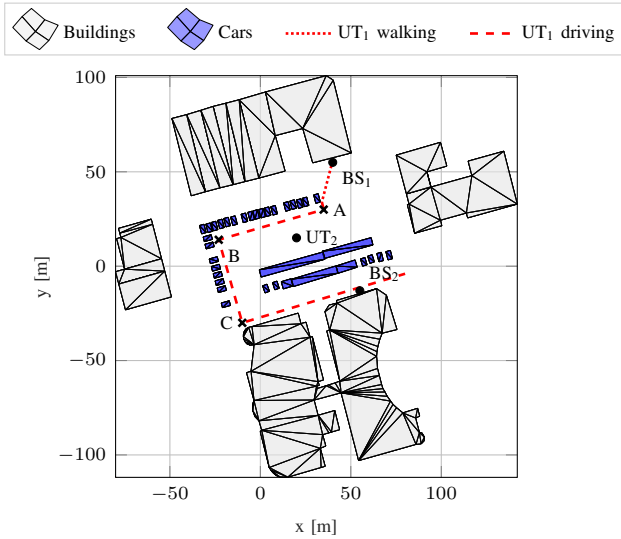
Fig. 1: Reference scenario.

Fig. 2: Temporal evolution of the signal strength experienced by UT_1.

TABLE I: Simulation parameters.

Frequency	28 GHz
Bandwidth	400 MHz
Channel sampling period	5 ms
NR numerology index	2
Transmission power	30 dBm
Noise figure	9 dB
Base Station (BS) array size	8×8
UT array size	$\{1 \times 4, 4 \times 1, 4 \times 4\}$
BS element pattern	{Isotropic, 3GPP, Cosine}
UT element pattern	Isotropic
BF algorithm	{SVD, Codebook}
Codebook BF period	{10, 100, 1000} ms
APP packet size	1490 bytes
Inter-packet interval	$\{10, 1000\}$ μs
RLC mode	Acknowledge Mode (AM)

for a given channel estimate, and some others even try to also take into account the interference generated to other users.

In general, two main approaches exist: those based on a channel estimate, and those based on BF codebooks.

For the first approach, we implemented an algorithm originally proposed in [20] based on the MIMO *Maximum Ratio Transmission* scheme, in which the optimal weight vectors corresponds to the singular vectors associated with the largest singular values of the Singular Value Decomposition (SVD) of the estimated channel matrix. For a perfect channel estimate in interference-free environments, this method ensures optimal performance. Unfortunately, good channel estimates are hard and expensive to obtain, especially when dealing with large antenna arrays. The SVD decomposition is itself an expensive operation, and sending feedback information comprises a difficult trade-off between accuracy and overhead. For this work, we assume that the channel matrix is perfectly known, thus posing the BF algorithm in ideal conditions.

For the second approach, we implemented a generic interface for codebooks, allowing the user to create custom ones. We also implemented a file-based codebook, allowing to create complex codebooks using custom and highly-specialized software, avoiding the computation of sophisticated algorithms on ns-3. As a first step, the implemented codebook-based BF computes the Signal to Interference plus Noise Ratio (SINR) for every pair of TX/RX BF vector, choosing the pair with the best performance. The advantages over the previous approach are many, in particular, no channel estimation nor complex matrix decomposition has to be performed and the only feedback needed is the index corresponding to the best performing BF codeword. On the other hand, exhaustive search among all possible codeword pairs may be inefficient, while reducing the search to a subset of codewords might yield sub-optimal performance. We leave a more realistic and standard-compliant beam-management implementation and evaluation as future work.
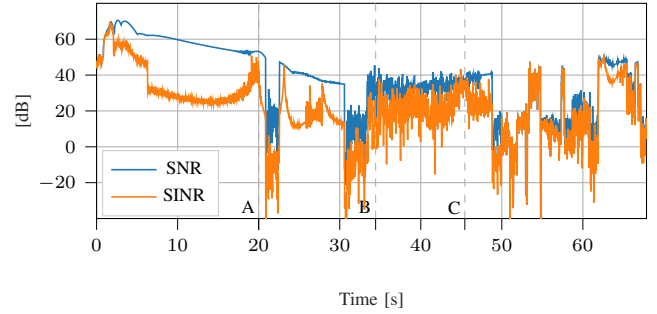
IV. SIMULATION SETUP

We carried out a simulation campaign to evaluate the performance of different antenna and BF configurations. To this aim, we used the ns-3 mmWave module extended with the proposed modeling framework. The scenario we considered, depicted in Fig. 1, models a parking lot with multiple cars (between 1.2 and 2.25 m high) and buildings, sampled every 5 ms. Two mmWave BSs providing cellular coverage are placed on the front face of two buildings at a height of 3 m and are oriented with a bearing angle in the direction normal to the wall and with a downtilt of 12° with respect to the horizon. Two users, UT_1 and UT_2, both at a height of 1.5 m, are connected to the respective BS. During the simulation, UT_1 leaves the main building walking at 1.2 m/s up to point A and then starts driving towards the exit of the parking lot at 4.2 m/s, while UT_2 stands still at the center of the scenario.

The same type of BF schemes is used by all nodes of the scenario. We assume perfect channel knowledge for SVD BF, computed for every received and transmitted packet. Instead, to assess the impact of realistic mobility on this type of scenario, codebook-based BF is only updated to find the best codeword pair for each TX/RX node pair every [10, 100, 1000] ms. Codebooks have been generated ensuring that adjacent beams cross at 3 dB below the maximum directivity and with no tapering across antennas.

The system operates at 28 GHz with a bandwidth of 400 MHz, and is configured with NR numerology index 2. The downlink traffic is generated by a remote server which transmits UDP packets to the users at a constant rate. Table I summarizes the parameters used in our evaluation.
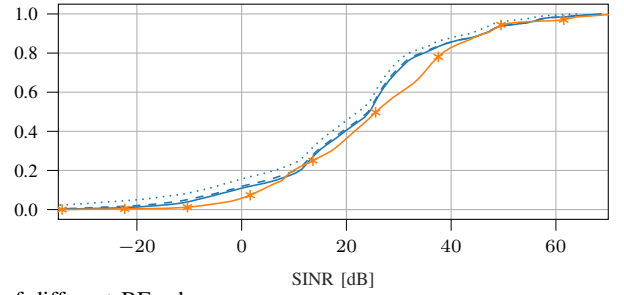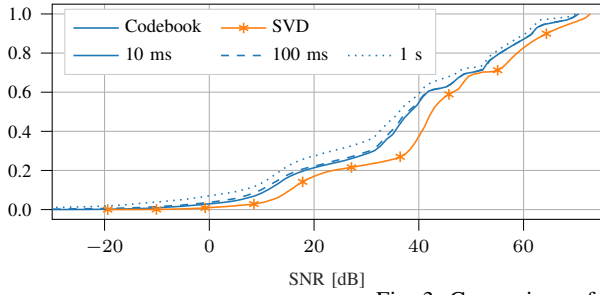
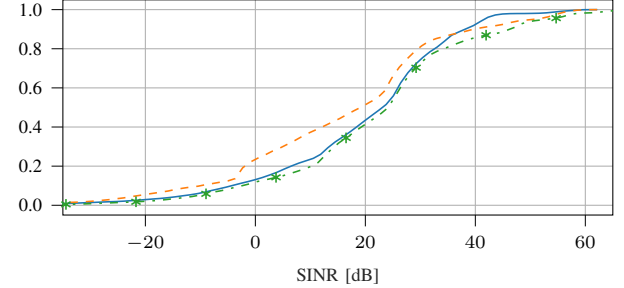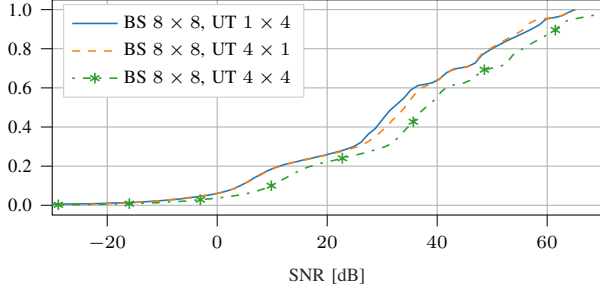Fig. 3: Comparison of the CDFs of different BF schemes.

Fig. 4: Comparison of the CDFs of different phased antenna array configurations at the UT side.

To evaluate the communication performance, we considered both link-level and end-to-end metrics, including SINR and Signal to Noise Ratio (SNR) experienced by UT_1, respectively showing the performance with and without the interference from the second cell, and APP-layer throughput.

V. SIMULATION RESULTS

In this section, we present and comment the results obtained. Unless explicitly stated, we consider the baseline simulation to have 4×4 arrays for the UTs, 3GPP antenna elements for the BSs, and codebook-based BF with 100 ms beam alignment, in addition to the parameters shown in Table I.

In Fig. 2, we reported the temporal evolution of the SNR and SINR experienced by UT_1. During the first part of the simulation, the SNR stays always above 50 dB and decreases as the user walks away, but the presence of interference strongly affects the channel quality, as shown by the behavior of the SINR. At time instant A, the user gets in its car and starts driving towards the exit of the parking lot. Shortly after 20 s and 30 s, some of the parked cars temporarily block the line of sight, making the channel quality suddenly drop. From time instant B to time instant C, both the SNR and the SINR show an oscillating behavior caused by the presence of multiple reflections with similar path losses from the surrounding cars. The last part of the simulation is characterized by multiple blockage events due to the cars parked in the bottom part of the parking lot. During this phase, the SNR and SINR exhibit similar behavior since the user is no longer subject to the inference caused by the communication between BS_2 and UT_2.

Fig. 3 shows the Cumulative Distribution Functions (CDFs) of SNR and SINR experienced by UT_1 with different BF configurations. We can notice that the SVD approach guarantees the best performance in terms of SNR, as supported by the theory, but not always when considering the SINR,

i.e., when interference is considered. Since SVD BF does not account for interference when computing the BF vectors, while codebook BF does so when probing the different codeword pairs, the performance gap between the two approaches is reduced and SVD may even be suboptimal, as shown in Section III-C. Moreover, it can be seen that the value of the refresh rate used to update the weight vectors affects the behavior of the codebook-based algorithm, providing better performance for more frequent updates. Due to the geometry of the environment and the mobility, diminishing returns are clearly visible when reducing the beam alignment period from 100 ms to 10 ms making the extra overhead unnecessary.

Fig. 4 shows a comparison between different array sizes for the UTs. Clearly, the most complex configuration represented by a 4×4 array is able to achieve the highest performance for both SNR and SINR. This is due both to the higher antenna gain obtained with the larger antenna array, but also to the reduced interference due to the higher directivity. On the other hand, considering vertical 4 elements Uniform Linear Arrays (ULAs) results in a very similar performance in the interference-free scenario, but vastly different performance when considering the interfering cell. In fact, a vertical array is only able to produce directivity with cylindrical symmetry around the vertical axis. Being both BSs at the same height, a good BF codeword able to improve the received power will also be likely to increase the downlink interference from the second cell. On the other hand, when orienting the linear array horizontally, the cylindrical symmetry will also rotate over the horizontal axis. In this case, the geometry of the environment and the positioning of the BSs makes it less likely to incur strong interference.

Fig. 5 evaluates the impact of the element radiation pattern on the SNR experienced by the user. Isotropic elements radiate equal power in all directions, and therefore provide a low
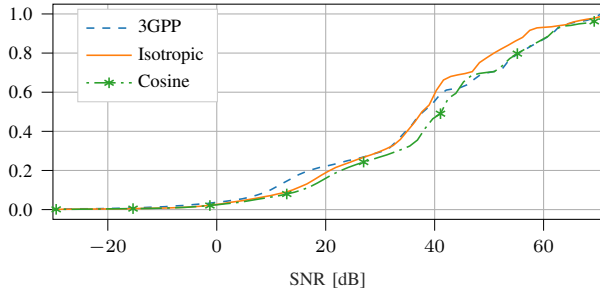
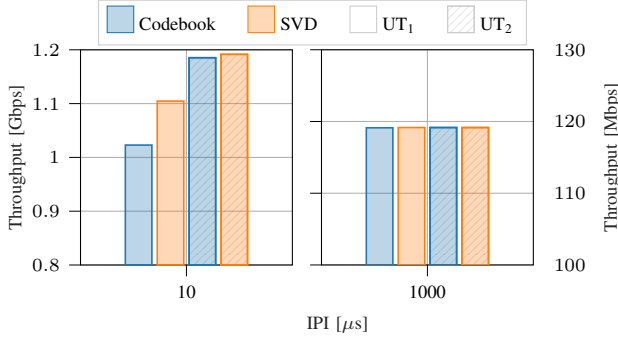Fig. 5: Comparison of the CDFs of different antenna element patterns.

Fig. 6: APP-layer throughput for different inter-packet intervals for a UDP stream.

directive gain but are able to cover a wide area. On the contrary, elements characterized by the 3GPP pattern have high directivity but small beamwidth, which implies that the transmitted power is focused in a small portion of the space. The best performance is achieved with the cosine pattern set to have a 3 dB beamwidth of $120°$, thus obtaining a maximum gain G_{max} =5.7 dBi, as this represents a good compromise between directivity and beamwidth.

Fig. 6 shows the average throughput achieved by UT_1 and UT_2 at the APP layer. With an inter-packet interval of 10 μs, the network is highly loaded and the scarcity of radio resources may prevent the recovery of the lost packets, e.g., by means of Medium Access Control (MAC) and Radio Link Control (RLC) layer retransmissions. In this situation, the choice of the BF algorithm may have a strong impact on the end-to-end performance, especially in the presence of user mobility. Indeed, as shown in Fig. 6, the higher channel gain provided by the SVD-based algorithm allows UT_1 to achieve higher throughput, while there is no benefit for UT_2 since it stays in the same position during the entire simulation. Instead, with a higher inter-packet interval, the codebook-based algorithm achieves the same performance as the SVD, since the recovery mechanisms at the MAC and RLC layers are able to compensate for the lower channel quality.

VI. CONCLUSIONS

In this paper we presented a modeling framework for the end-to-end evaluation of 5G mmWave cellular networks which is compliant with the 3GPP NR specifications. Our work extends the capabilities of the ns-3 mmWave module presented in [8] by providing (i) a ray-tracing based channel model for mobile users, which improves the spatio-temporal coherence over the previous stochastic channel [7], (ii) a flexible antenna module, comprising multiple parametric antenna elements as well as a generic interface for phased antenna arrays, and (iii) a BF module supporting different algorithms for the computation of the optimal BF vectors. Using this framework, we evaluated the performance achieved by different antenna configurations and BF schemes in a realistic simulation scenario. Our results show that inaccurate antenna and BF designs may provide sub-optimal channel gains and affect the performance of the higher layers. As future work, we plan to extend the proposed framework with a more realistic beam-management implementation, to account for the overhead introduced by beam search operations.

REFERENCES

[1] 3GPP, "NR and NG-RAN Overall Description," TS 38.300 (Rel. 15), 2018.

[2] ——, "New WID on extending current NR operation to 71 GHz," Qualcomm, RP-193229 - 3GPP TSG RAN Meeting 86, Dec. 2019.

[3] S. Rangan, T. S. Rappaport, and E. Erkip, "Millimeter-wave Cellular Wireless Networks: Potentials and Challenges," *Proceedings of the IEEE*, vol. 102, no. 3, pp. 366–385, Mar. 2014.

[4] V. Va and R. W. Heath, "Basic Relationship between Channel Coherence Time and Beamwidth in Vehicular Channels," in *IEEE 82nd Vehicular Technology Conference (VTC2015-Fall)*, Boston, MA, USA, Sep. 2015.

[5] M. Giordani, M. Polese, A. Roy, D. Castor, and M. Zorzi, "A Tutorial on Beam Management for 3GPP NR at mmWave Frequencies," *IEEE Communications Surveys Tutorials*, vol. 21, no. 1, pp. 173–196, Sep. 2019.

[6] T. Zugno, M. Polese, M. Lecci, and M. Zorzi, "Simulation of Next-Generation Cellular Networks with Ns-3: Open Challenges and New Directions," in *Workshop on Next-Generation Wireless with Ns-3 (WNGW)*, Florence, Italy, Jun. 2019.

[7] T. Zugno, M. Polese, N. Patriciello, B. Bojović, S. Lagen, and M. Zorzi, "Implementation of a Spatial Channel Model for Ns-3," in *Workshop on ns-3 (WNS3)*, Gaithersburg, MD, USA, Jun. 2020.

[8] M. Mezzavilla, M. Zhang, M. Polese, R. Ford, S. Dutta, S. Rangan, and M. Zorzi, "End-to-End Simulation of 5G mmWave Networks," *IEEE Communications Surveys & Tutorials*, vol. 20, no. 3, pp. 2237–2263, Third Quarter 2018.

[9] M. Polese and M. Zorzi, "Impact of Channel Models on the End-to-End Performance of Mmwave Cellular Networks," in *IEEE 19th International Workshop on Signal Processing Advances in Wireless Communications (SPAWC)*, Kalamata, Greece, Jun. 2018.

[10] M. Lecci, P. Testolina, M. Polese, M. Giordani, and M. Zorzi, "Accuracy vs. Complexity for mmWave Ray-Tracing: A Full Stack Perspective," https://arxiv.org/abs/2007.07125.

[11] M. Lecci, M. Polese, C. Lai, J. Wang, C. Gentile, N. Golmie, and M. Zorzi, "Quasi-Deterministic Channel Model for mmWaves: Mathematical Formalization and Validation," in *IEEE Global Telecommunications Conference (GLOBECOM) (to be presented)*, Taipei, Taiwan, Dec. 2020.

[12] "Quasi-deterministic mmWave Channel Simulator." [Online]. Available: https://github.com/wigig-tools/qd-realization

[13] "ns-3 add-on for trace-based channel models." [Online]. Available: https://github.com/signetlabdei/qd-channel

[14] C. A. Balanis, *Antenna Theory: Analysis and Design*. Wiley-Interscience, 2005.

[15] M. S. Rabbani and H. Ghafouri-Shiraz, "Size Improvement of Rectangular Microstrip Patch Antenna at Mmwave and Terahertz Frequencies," *Microwave and Optical Technology Letters*, vol. 57, no. 11, pp. 2585–2589, Aug. 2015.

[16] Y. M. Abdelkader, M. M. Hamada, and A. N. Mohieldin, "System Level Co-Simulation Approach for Ultra-Wideband Massive MIMO Beam Forming Phased Array Transmitters," in *31st International Conference on Microelectronics (ICM)*, Cairo, Egypt, Egypt, Mar. 2019.

[17] Y. J. Cho, G. Suk, B. Kim, D. K. Kim, and C. Chae, "RF Lens-Embedded Antenna Array for mmWave MIMO: Design and Performance," *IEEE Communications Magazine*, vol. 56, no. 7, pp. 42–48, Jul. 2018.

[18] C. Menudier, J. Lintignat, S. Mons, P. Médrel, N. Delhote, E. Ngoya, S. Bila, M. Thévenot, B. Jarry, P. Gamand, J. Sombrin, and D. Baillargeat, "Design and optimization of multielement antennas and RF circuits for beamforming with a reduced number of RF Front-ends," in *IEEE MTT-S International Microwave Workshop Series on 5G Hardware and System Technologies (IMWS-5G)*, Dublin, Ireland, Aug. 2018.

[19] 3GPP, "Study on channel model for frequencies from 0.5 to 100 GHz," 3rd Generation Partnership Project (3GPP), Technical Report (TR) 38.901, Jun. 2018, version 15.0.0.

[20] M. Zhang, M. Polese, M. Mezzavilla, S. Rangan, and M. Zorzi, "ns-3 Implementation of the 3GPP MIMO Channel Model for Frequency Spectrum above 6 GHz," in *Workshop on ns-3 (WNS3)*, Porto, Portugal, Jun. 2017.